Intensity dependence of free-free absorption

1971 J. Phys. A: Gen. Phys. 4 574

(http://iopscience.iop.org/0022-3689/4/4/021)

J. Phys. A: Gen. Phys., 1971, Vol. 4. Printed in Great Britain

Intensity dependence of free–free absorption

M. B. NICHOLSON-FLORENCE

Department of Physics, University of Essex, Colchester, Essex, England

MS. received 29th December 1970

Abstract. The net absorption coefficient allowing for stimulated emission in a nonrelativistic plasma is calculated using the cross sections found by Bunkin and Fedorov. The computations range over many values of their two parameters, which are determined by the initial electron velocity and the frequency and intensity of the electromagnetic field. The energy absorbed is found at strong enough flux to decrease with increasing flux and to be primarily determined by single photon processes for all parameter values considered.

1. Introduction

In a previous paper by Hughes and Nicholson-Florence (1968, to be referred to as I) the intensity dependence of the inverse bremsstrahlung absorption coefficient was discussed. The exact form of that dependence will influence the choice of parameters in attempts to achieve hot dense plasmas for fusion research by irradiation with intense laser fluxes. In I two forms of intensity dependence were shown at high flux intensity D, one deriving from a semiclassical viewpoint, the other an extension to the work of Rand (1964). The former gave a dependence of the form $D^{-1/2}$, the latter $D^{-3/2}$. The difference was ascribed to the neglect of multi-photon contributions in the former derivation and their inclusion in the latter. In order to assess the validity or otherwise of this conclusion and to attempt to find a more satisfactory estimate of the absorption coefficient, calculations have been undertaken based on the cross sections for n-photon stimulated emission and absorption given by Bunkin and Fedorov (1966) for an electron scattered by an ion in an electromagnetic field. These have indicated an absorption coefficient basically agreeing with Rand's result and have shown that the difference between the two previous results does not depend upon multi-photon effects but rather lies in the different phase factors in the calculations. These phase factors affect the time averaging implicit in an absorption coefficient, but their significance is not clear.

2. Previous work

The classical (weak field) absorption coefficient α_{FF} for an electron scattered by an ion within an electromagnetic field is obtained using the first Born approximation for the ion scattering potential and the first-order perturbation theory approximation in the electromagnetic field. At high fields such a perturbation expansion is not valid; a method is required independent of electromagnetic field strength, treating the ion scattering as the only perturbation.

Rand sought such a method. Using an oscillating coordinate system, he solved the Schrödinger equation for the motion of an electron scattered by an ion and determined the energy absorbed from an electromagnetic field by equating it with the work done on the oscillating ion by longitudinal waves in the electron probability cloud. The result quoted (α_{RL}) was for a low velocity electron such that its mean kinetic energy $\frac{1}{2}mv_0^2$ was less than the photon energy $h\nu$.

The result quoted can be written

$$\alpha_{\mathrm{RL}} = \frac{16\pi^2 n_e n_i Z^2 e^4}{cmE_0^2}\left\langle \frac{u_0^2 \sin^2 2\pi\nu t}{(u_0^2+v_0^2)^{3/2}} \ln\left(\frac{8mu^2}{h\nu}\right)\right\rangle$$
$$= \frac{32\pi^2 n_e n_i Z^2 e^3}{c}\frac{\nu}{E_0^3} \ln(\gamma\xi) \ln\left(\frac{64\gamma}{\xi}\right)$$

where the angle brackets indicate a time average,

$$\xi = h\nu/mv_0^2 \gg 1$$
$$\gamma = ev_0E_0/2\pi h\nu^2$$
$$u = u_0 \sin 2\pi\nu t$$

and

$$u_0 = eE_0/2\pi m\nu$$

is the directed velocity amplitude.

Hughes and Nicholson-Florence extended this result in I to the case where $\xi \ll 1$, and obtained

$$\alpha_{\mathrm{RH}} = \frac{32\pi^2 n_e n_i Z^2 e^3}{c}\frac{\nu}{E_0^3} 4 \ln(4\gamma\xi).$$

They also considered the problem from a quasi-classical viewpoint, expressing the instantaneous absorption coefficient as a function of electron velocity and then simply estimating the instantaneous electron velocity in a strong field and averaging over a cycle of the field oscillation.

The instantaneous nett absorption coefficient for a precise total electron velocity v was

$$\frac{4n_e n_i Z^2 e^6}{3m^3 c\nu^2 v^3} \ln\left(\frac{2mv^2}{h\nu}\right)$$

and if

$$v^2 = v_0^2 + u^2$$

that is, assuming a strong field at right angles to the random electron velocity v_0, then taking a radiation energy flux of $(E_0^2 c/4\pi)\cos^2 2\pi\nu t$ and time averaging the absorption gave an absorption coefficient

$$\alpha_{\mathrm{E}} = \frac{8n_e n_i Z^2 e^6}{3m^3 c\nu^2 E_0^2}\left\langle \frac{E_0^2 \cos^2 2\pi\nu t}{(u^2+v_0^2)^{3/2}} \ln\left(\frac{2mv^2}{h\nu}\right)\right\rangle$$
$$= \frac{16n_e n_i Z^2 e^6}{3\pi m^3 c}\frac{1}{\nu^2 u_0^3}\int_0^{\pi/2} \frac{\cos^2\theta}{(\sin^2\theta + a^2)^{3/2}} \ln\left(\frac{2mv^2}{h\nu}\right) \mathrm{d}\theta$$

where

$$a = v_0/u_0, \theta = 2\pi\nu t.$$

This reduced for $a \ll 1$, for strong fields, to

$$\alpha_{\mathrm{E}} = \frac{32}{3}\frac{n_e n_i Z^2 e^5}{m^2 c}\frac{1}{\nu v_0^2 E_0} \ln\left(\frac{2}{\xi}\right).$$

The difference between α_E and α_{RH} is seen to be essentially the substitution of v_0 in α_E by u_0 in α_{RH}, thereby changing the frequency, field and initial velocity dependences. This is a consequence of the appearance of $\cos^2\theta$ in α_E as compared to $\sin^2\theta$ in α_{RH} before time averaging.†

In order to clarify the intensity dependence of the absorption coefficient, calculations were performed based on work done by Bunkin and Fedorov. These authors considered the wave function of a spinless, nonrelativistic electron in a classical electromagnetic field in the dipole approximation. Ignoring spontaneous transitions, they determined the cross sections for absorption and induced emission of a photon due to the perturbation of an ionic Coulomb potential in the Born approximation. Except for the weak field case, these cross sections could not be integrated over all angles analytically but only by numerical methods.

3. Computations

We consider the process in which a free electron of initial momentum $m\bar{v}_0$ along Oz gains energy $nh\nu$ from the laser beam (n is a positive or negative integer) as it is

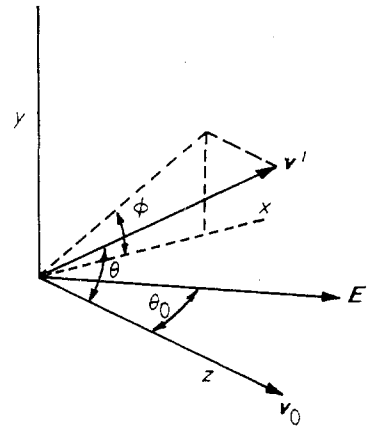

Figure 1. The kinematics of free-free absorption.

scattered by an ion into momentum $m\boldsymbol{v}'$ as in figure 1. The cross sections for this process, as given by Bunkin and Fedorov, are

$$\frac{d\sigma^n(\theta_0)}{d\Omega_0} = \frac{2m^2v_0h\nu n_i}{\pi\hbar^4E_0^2c}\Phi_n$$

$$\Phi_n = \int d\Omega \left| \int d^3\boldsymbol{r}\, V(\boldsymbol{r}) \exp\left\{ i\frac{m}{\hbar}(\boldsymbol{v}_0 - \boldsymbol{v}').\boldsymbol{r} \right\} \right|^2 \lambda J_n^2(\eta)$$

$$\eta = \gamma\cos\theta_0(1-\lambda\cos\theta) - \gamma\lambda\sin\theta_0\sin\theta\cos\phi.$$

$V(\boldsymbol{r})$ is the ion potential, $d\Omega$ is the element of solid angle around $\boldsymbol{v}'$ into which the electron is scattered ($d\Omega = \sin\theta\, d\theta\, d\phi$), $d\Omega_0$ around $\boldsymbol{v}_0$. J_n is the nth order Bessel function and $\lambda^2 = 1+2n\xi = (v'/v_0)^2$. The angle θ_0 is the angle between the electric field $\boldsymbol{E}$ and the vector $\boldsymbol{v}_0$. In a physical case one might well expect the angle θ_0 to be distributed at random at least initially in the heating process.

† Note: In I figures 1(*a*) and (*b*) are plots of $\alpha D/n_e n_i Z^2 e^6$; the factor e^6 was omitted in printing.

Substituting a Coulomb potential for $V(r)$ we have

$$\frac{\mathrm{d}\sigma^n(\theta_0)}{\mathrm{d}\Omega_0} = \frac{8\pi Z^2 e^4 n_i h\nu}{m^2 c E_0{}^2 v_0{}^3} I_n(\theta_0) \equiv A(\nu, E_0, v_0)\, I_n(\theta_0, \gamma, \xi)$$

with

$$I_n(\theta_0) = \int \frac{J_n{}^2(\eta)\,\mathrm{d}\Omega}{\lambda(\cos\theta - b)^2}$$

where

$$b = \frac{(1+\lambda^2)}{2\lambda}.$$

Also

$$\sigma^n = \tfrac{1}{2}\int_0^{\pi} \mathrm{d}\sigma^n(\theta_0) \sin\theta_0\, \mathrm{d}\theta_0 = A(\nu, E_0, v_0)\, S_n(\gamma, \xi)$$

with

$$A(\nu, E_0, v_0) = \frac{8\pi Z^2 e^4 n_i h}{m^2 c} \frac{\nu}{E_0{}^2 v_0{}^3} \qquad \text{and} \qquad S_n(\gamma, \xi) = \int_0^{\pi/2} I_n(\theta_0) \sin\theta_0\, \mathrm{d}\theta_0$$

if all θ_0 are equally probable.

Values of $\mathrm{d}\sigma^n(\theta_0)$ and σ^n were calculated using an ICL 1900 computer, evaluating values of $I_n(\theta_0)$ for various values of γ and ξ. These values were chosen to give a series of values of $\mathrm{d}\sigma^n(\theta_0)$ and σ^n for various values of γ and ξ including combinations for constant $\gamma^2\xi \sim E_0{}^2$ or constant $\xi^2\gamma \sim E_0 v_0{}^{-3}$ or constant $\gamma\xi \sim u_0 v_0{}^{-1}$.

Two programs were used. One employed Simpson's rule and a choice of three fixed step lengths, was economical in time but utilized only the order of a thousand points per $\mathrm{d}\sigma^n(\theta_0)$ value in the order of one minute. The second programme used a six point Gaussian fit with variable step-length and was more accurate utilizing hundreds of thousand of points requiring tens of minutes per $\mathrm{d}\sigma^n(\theta_0)$ value despite faster computations. A typical plot of computed values of $I_n(\theta_0)$ against θ_0 is shown in figure 2 for different values of n, γ and ξ.

The two computation methods gave agreement over the region considered here. Reliability decreased with increasing γ and decreasing ξ. Typically there would be γ oscillations in $J_n(\eta)$ in one complete integration interval; this would necessitate at least γ points per integration. But even only allowing for 1% confidence a γ of 100 would require two hours to compute for a particular n and ξ. Limited computing time curtailed extension to much larger values of γ. Moreover, the desired absorption coefficient is proportional to the sum of the nett n-photon absorption coefficients that is

$$\alpha^n = n_e(\sigma^{|n|} - \sigma^{-|n|}).$$

At high γ and low ξ the difference between $\sigma^{|n|}$ and $\sigma^{-|n|}$ becomes a small proportion of $\sigma^{|n|}$ and comparable to the computational uncertainty. Accordingly the results presented are limited to $\gamma \ll 10^2$, $\xi \gg 10^{-2}$. Figure 3 shows a plot of σ^1 and σ^{-1} for various γ and ξ.

For a given mean flux $D = E_0{}^2 c/8\pi$ we desire to know the power absorbed due to an n-photon process $\alpha^n D$. For the particular case of the Neodymium 1·06 μm laser we have

$$\frac{\alpha^n D}{n_e n_i Z^2 e^6} = 5{\cdot}26 \times 10^{37} \xi^{3/2} S_n'(\xi, \gamma) \qquad (\mathrm{erg\ cm^3\ s^{-1}})$$

where

$$S_n' = S_{|n|} - S_{-|n|}$$

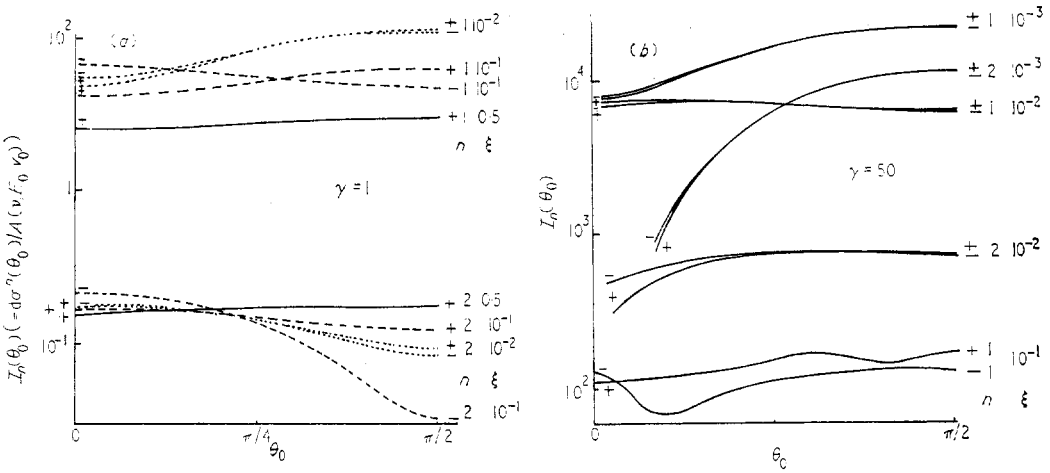

Figure 2. Typical plots of $I_n(\theta_0)$ against θ_0 for various n, γ and ξ: (*a*) $\gamma = 1$; (*b*) $\gamma = 50$.

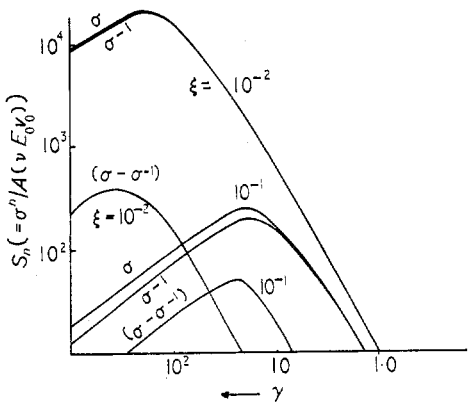

Figure 3. Plot of $S_n(\gamma, \xi)$ against γ for $n = \pm 1$ for $\xi = 10^{-1}$ and 10^{-2}. (Note: for σ read σ^{+1}.)

and note that at 1·06 μm

$$D = 2{\cdot}79 \times 10^{19}\gamma^2\xi \qquad (\text{erg cm}^{-2}\,\text{s}^{-1}).$$

4. Results

In figure 4 are shown the curves of absorbed power $\alpha^n D/n_e n_i Z^2 e^6$ at 1·06 μm for various values of the parameters n, γ and ξ. These are transcribed in figures 5, 6 and 7 into values of $\alpha^n D/n_e n_i Z^2 e^6$ for different n, ξ and $\gamma^2\xi$, the flux parameter. For constant frequency, ξ^{-1} measures initial electron energy and at the neodymium laser frequency is approximately the value in electron volts ($h\nu_{Nd} = 1{\cdot}17$ eV).

Figure 5 is a plot of absorbed power $\alpha^n D/n_e n_i Z^2 e^6$ for constant initial electron energy and constant frequency (ξ constant, $\nu = \nu_{Nd}$). For fast electrons ($\xi < 1$)$\alpha^1 D$ is linear provided the directed component of electron velocity u_0 is less than the

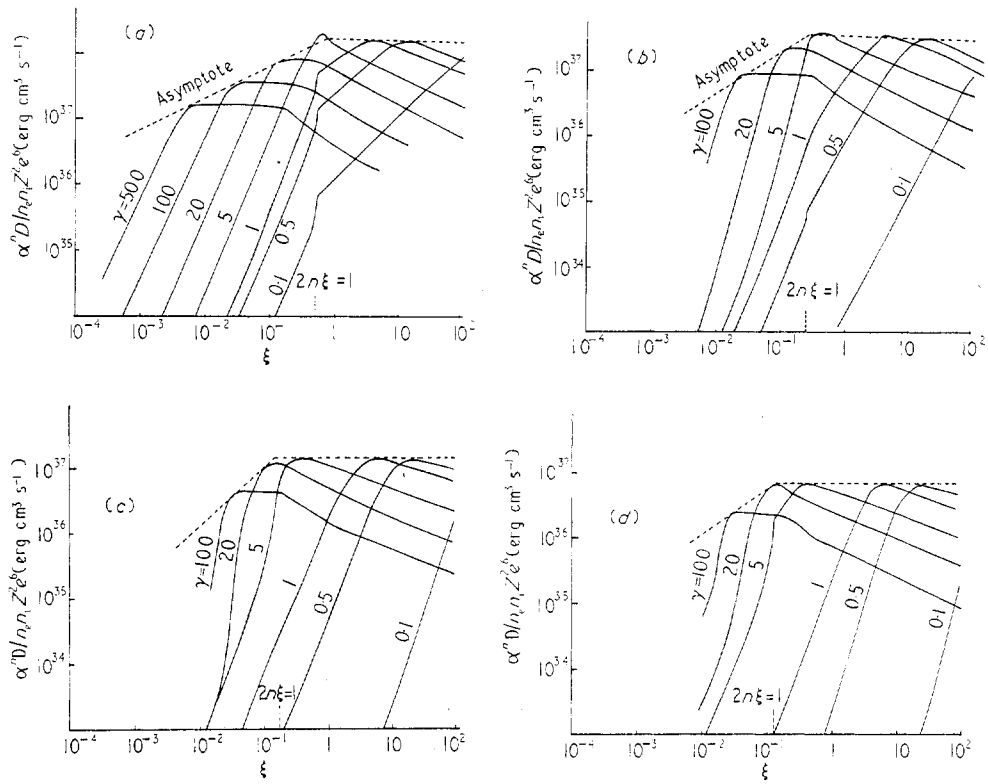

Figure 4. Curves of absorbed power at 1·06 μm for various n, γ and ξ: (*a*) $n = 1$; (*b*) $n = 2$, (*c*) $n = 3$, and (*d*) $n = 4$.

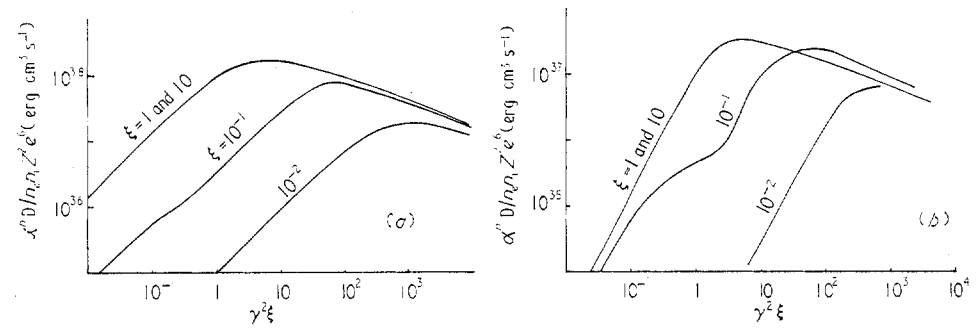

Figure 5. Curves of absorbed power at 1·06 μm at constant initial electron velocity against flux $\gamma^2\xi$ for (*a*) $n = 1$, (*b*) $n = 2$.

initial random or thermal velocity $v_0(\gamma\xi < 2)$. For slow electrons ($\xi > 1$)$\alpha^1 D$ is linear provided the flux $\gamma^2\xi < 1$. The equivalent plots for $n = 2$, 3, 4 in these regions show the expected D^n dependence of $\alpha^n D$. For fast electrons ($\xi < 1$), where $u_0 > 2v_0$ or $\gamma\xi > 2$ and for slow electrons ($\xi > 1$) where the flux is high, $\gamma^2\xi > 1$, the values of $\alpha^n D$ are basically similar for different n having the same form, decreasing with increasing flux D as $D^{-1/2}$ to $D^{-1/3}$ and being virtually independent of ξ. The treatment due to Rand would predict a $D^{-1/2}$ dependence. The curves for $\xi > 1$ merge.

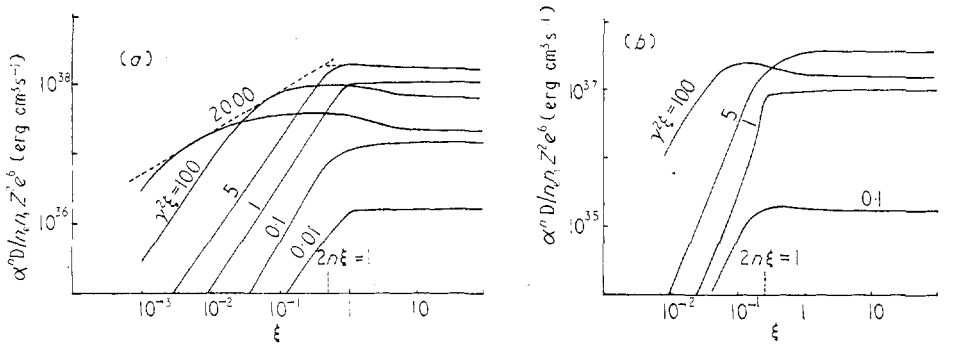

Figure 6. Curves of absorbed power at constant flux against ξ for (*a*) $n = 1$, (*b*) $n = 2$.

Figure 6 shows the plot of absorbed power $\alpha^n D/n_e n_i Z^2 e^6$ against initial electron energy ξ at constant frequency ν_{Nd} and flux $\gamma^2\xi$. The independence of $\alpha^n D$ with respect to ξ is apparent for $u_0 > 2v_0$ or $\gamma\xi > 2$ and for $mv_0^2 > h\nu$, $\xi > 1$. When these inequalities do not apply we have $\alpha^1 D \propto \xi^{3/2}$ and $\alpha^2 D \propto \xi^{5/2}$. That is $\alpha^1 \propto v^{-3}$ and $\alpha^2 \propto v^{-5}$. For high fluxes $\gamma^2\xi > 1$ between $\xi = 1$ and $\gamma\xi \sim 2$ there is a broad maximum of absorbed flux merging into the ξ-independent region of $\xi > 1$. An envelope is evident limiting the maximum power absorption at the frequency chosen. For $n = 1$, this is a line varying at something between $\xi^{1/2}$ and $\xi^{3/5}$ for $\xi < 1$, becoming independent of ξ for $\xi > 1$. Similarly there is an envelope for $n = 2, 3, 4$. The maximum absorbed power occurs for $n = 1$ at $\gamma^2\xi \sim 4$ with $\xi \geqslant 1$. For a specified flux $\gamma^2\xi$, however, maximum absorption power occurs at $n\xi \sim 1$ for each n. For a given ξ the maximum occurs for $n = 1$ and $\gamma\xi \sim 2$.

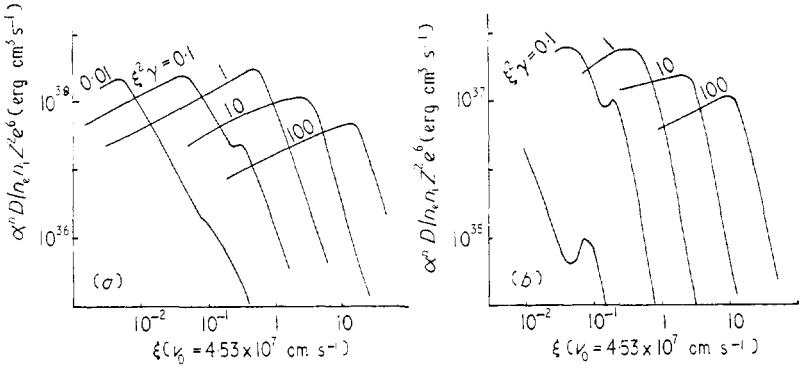

Figure 7. Curves of absorbed power at constant initial electron velocity (when $\xi \propto v$) for (*a*) $n = 1$, (*b*) $n = 2$, to demonstrate frequency dependence. In (*b*) the unlabelled curve is for $\xi^2\gamma = 0{\cdot}01$.

Figure 7 shows the frequency dependence of $\alpha^n D$ for a constant initial electron velocity of $4{\cdot}53 \times 10^7$ cm s^{-1}, chosen for convenience so that $mv_0^2 = h\nu_{Nd}$. The dependence is of the form $\nu^{-3n-1/2}$ for weak fields with $\gamma < 1$ and for slow electrons ($n\xi > 1$); but for slightly stronger fields with $\gamma\xi < 2$ or $u_0 < 2v_0$, for fast electrons ($n\xi < 1$) this changes to ν^{-2} for $n = 1$, and ν^{-3} for $n = 2$, (data was insufficient to

indicate corresponding dependence for $n = 3, 4$). Finally for strong fields with $\gamma\xi > 2$, $u_0 > 2v_0$, this becomes a dependence of $\nu^{1/4}$ to $\nu^{1/2}$ contrasting with Rand's linear dependence on frequency ν at high flux.

All these graphs have a basic similarity for $n = 1, 2, 3, 4$ with a consistent decrease in magnitude of $\alpha^n D/n_e n_i Z^2 e^6$ for increasing n. Apparently, the dominant absorption process is always the single photon process even at high fields since the D^n dependence holds only for $\gamma^2\xi < 1$ or $\gamma\xi < 2$; that is, where the kinetic energy of the directed motion is less than the photon energy or the directed velocity is less than the random velocity of the electron initially. The curves all increase to a maximum and decrease with increasing flux, the maxima falling off with n a little more rapidly than n^{-2}.

Figure 8 compares the absorbed energy $\alpha^1 D/n_e n_i Z^2 e^6$ for Nd laser and CO_2 laser radiation at three flux levels. At low flux the expected $\nu^{-7/2}$ or ν^{-2} dependence gives rise to significantly more absorption per unit densities for CO_2 laser radiation at 10·6 μm than for Nd laser radiation at 1·06 μm. But because of the ν^{-3} dependence of $\gamma^2\xi$, the CO_2 radiation reaches the maximum absorption at lower fluxes than Nd and when $\gamma^2\xi$ for Nd reaches unity, the $\gamma^2\xi$ corresponding for CO_2 is 10^3 and the absorption, except for large enough velocities, becomes frequency-independent.

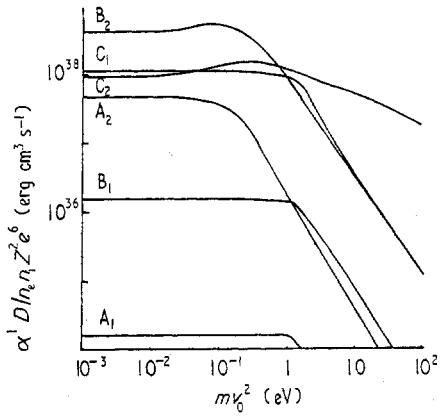

Figure 8. Comparison of absorbed energy ($n = 1$) for Nd and CO_2 laser irradiation at three flux levels. Values of $\gamma^2\xi$, for Nd: (A1) = 10^{-4}, (B1) = 10^{-2}, (C1) = 1; for CO_2: (A2) = 10^{-1}, (B2) = 10, (C2) = 10^3.

5. Conclusions

The computations for $d\sigma^n(\theta_0)$ the differential cross sections for particular values of θ_0, as shown in figure 2, reveal that the nett absorption may only be a small fraction of the total absorption before taking into account the stimulated emission. The multiphoton ($n = 2, 3, 4$) contributions to the nett absorption are always smaller than the one photon contribution but bear a general resemblance to it. The contributions $n = 1$ to 4 may be added to give a total nett absorption which will be very similar to the one-photon absorption with an additional factor of the order of two.

Except for slow electrons ($\xi \geqslant 1$), for all $n = 1$ to 4 the tendency is for emission to exceed absorption when the initial electron velocity is nearly parallel to the electric field vector, that is for small θ_0, and the reverse for θ_0 approaching $\pi/2$, when the

electron velocity is perpendicular to the field. This agrees with the result due to Marcuse (1962). Any marked variation in the electron velocity angular distribution from the isotropic one assumed here may cause a significant change in the nett absorption. There will be a tendency towards more absorption if the proportion of electrons with velocities perpendicular to the electric field is enhanced and towards nett emission if that for velocities parallel to the electric field is enhanced.

The computations of σ^n and $\alpha^n D$ are in general agreement with the results obtained using Rand's treatment rather than the semiclassical model of I. With the power absorbed depending on the high flux D as $D^{-1/2}$, the considerations of I concerning an optimum flux for plasma heating and minimum times and masses to achieve specified temperatures of plasma apply. The transition from the linear regime to the $D^{-1/2}$ regime occurs when the directed component of the electron velocity becomes comparable with the random component and will occur at lower electron velocities and temperatures for lower frequencies. The optimum power absorbed per unit plasma volume, however, at a given density (n_e, n_i) is independent of frequency apart from a logarithmic term. Nevertheless, if the plasma is of a given size and a density initially such that the plasma frequency equals the laser frequency, the maximum temperature attained will increase linearly with frequency.

In a real plasma, important cooperative effects will occur between electrons. These have not been discussed in the present paper and are best treated by a kinetic theory approach as used in Silin (1965) and Kaw and Salat (1968). Furthermore, other nonlinear effects are being studied which have the result of increasing absorption for radiation in a narrow frequency interval near the plasma frequency and therefore enhance absorption on the density beach of an overdense plasma. Kaw and Dawson (1969) have discussed various forms of ion-wave instabilities which will amplify plasma fluctuations to produce large amplitude ion waves and may enhance absorption around the plasma frequency by a few orders of magnitude. Further study is desirable on these instabilities with intense fields ($\gamma\xi > 2$) and to assess the relative importance of the collective effects as against the single ion–electron encounter treatment in this paper which holds for frequencies greater than the plasma frequency.

References

Bunkin, F. V., and Fedorov, M. V., 1966, *Sov. Phys.—JETP*, **22**, 844–7.
Hughes, T. P., and Nicholson-Florence, M. B., 1968, *J. Phys.* A: *Gen. Phys.*, 588–95.
Kaw, P. K., and Dawson, J. M., 1969, *Phys. Fluids*, **12**, 2586–91.
Kaw, P. K., and Salat, A. R., 1968, *Phys. Fluids*, **11**, 2223–32.
Marcuse, D., 1962, *Bell Syst. Tech. J.*, **41**, 1557–71.
Rand, S., 1964, *Phys. Rev.*, **136**, B 231–7.
Silin, V. P., *Sov. Phys.—JETP*, **20**, 1510–7.